Int J Adv Manuf Technol
DOI 10.1007/s00170-013-5593-6

ORIGINAL ARTICLE

A robust visual servo control system for narrow seam double head welding robot

Haiyong Chen · Kun Liu · Guansheng Xing · Yan Dong · Hexu Sun · Wei Lin

Received: 17 May 2013 / Accepted: 23 December 2013

Abstract In this paper, an image-based visual servo control system is developed and integrated into a double head welding robot for CO_2 gas shielded arc welding, which is mainly used to weld the narrow seam whose width is generally less than 0.2 mm. Firstly, a robust and reliable image processing algorithm is presented to reliably extract the seam feature during the welding. A statistic-based filter method is proposed to effectively weaken the image noises caused by various disturbances. The region of interest (ROI) of the image is determined to improve the efficiency and reliability of the image processing. The feature line of the narrow seam is extracted by combining the technique of the least-square line fitting with the Hough transform method. Secondly, a visual servo control system is designed to realize accurate tracking and initial point localization of the narrow seam. Moreover, an image error filter and output pulse verification are utilized to guarantee the reliability and stability of the control system. Finally, a series of experiments with real welding robots are conducted in the production line of a container manufacturing factory, demonstrating the satisfactory performance and high welding quality of the proposed visual servo control system.

H. Chen · K. Liu · G. Xing · Y. Dong · H. Sun
Control Science and Engineering, Hebei University of Technology, Tianjin 300130, China

H. Chen
e-mail: haiyong.chen@hebut.edu.cn

W. Lin (✉)
Department of Electrical Engineering and Computer Science, Case Western Reserve University, Cleveland, OH 44106, USA
e-mail: linwei@cwru.edu

W. Lin
Harbin Institute of Technology (Shenzhen Graduate school), Shenzhen, China

Published online: 25 January 2014

Keywords Servo control systems · Vision control · Seam tracking · Industrial robot · Container manufacturing · Laser welding

1 Introduction

In the past 30 years, welding robots have been an important and popular research topic in the manufacturing industry because they can prominently enhance the quality and production efficiency, improve work circumstance, and reduce work intensity of welders. Recently, many welding fields such as shipbuilding, container manufacturing, and pipe manufacturing were facing increasing dynamics of innovations, shortened product life cycles, and a continuing diversification of the product range [1–3]. Furthermore, the shortage and high cost of skilled workers are becoming a challenging and serious issue. They are a primary driving force in pushing employers to widely adopt intelligent weld robot systems in manufacturing, and in turn gaining advantages in the production quality and fierce market competition.

Until now, most of the industrial robots used in factory have still been under the work mode named by the "teaching-and-playback type". This type of welding robots has a strict accuracy demand on the position and shape of the weld seam. Therefore, it is difficult to provide a desired adaptive capacity to the changes of seam status, arc light, and splash disturbances during welding process [4]. In particular, in the field of narrow butt seam welding, it is usual for the workers to watch the seam under the strong arc environment, and then manually adjust the welding torch to align the welding seam during the welding process. As a consequence, it is not easy to guarantee the welding accuracy and efficiency because a long manually adjusting process is tedious, harmful, and burdensome for the welders [5]. To solve these problems, an intelligent seam sense and tracking method of welding robotic systems was

proposed, making it possible to reduce the effects of various seam errors and improve the quality of the narrow welded joints [6–8].

Sensors play a crucial role in a welding robotic system. So far, various types of sensors have been employed in industrial welding robots, such as inductive sensors, ultra sonic sensors, and vision sensors [9–11]. Among them, vision sensor systems have been employed to capture and understand welding seams due to their non-contact attribution, high accuracy, and abundant information. In the papers [12–14], researchers used the vision sensors to inspect and memorize the seam position before the welding and then, utilize the information to guide the torch to align the seam. The advantage of such methods is that the vision sensor information replaces manual teaching, and thus shortening the teaching time and quickly obtaining the seam position, in a robust and reliable manner.

In the case when the narrow seam is under consideration, the aforementioned methods such as teaching-and-replay or the approach based on vision sensors are difficult to achieve a desirable accuracy because the bigger error may be rendered by thermal distortions of the welding process [13]. Although the off-line teaching using a vision sensor can alleviate the problem of gaining the accurate seam path, it has certain drawbacks [4, 8, 12, 13]. Firstly, the geometries of the actual workpiece to be welded may not be represented accurately by one seam path because of the existence of the large machining tolerance and assembly error. Secondly, with the aid of the sophisticated electrical and mechanical equipments, even if the precise assembly can meet the welding requirements, the cost is perhaps too high and unprofitable for small- and median-sized welding applications. Thirdly, the actual hardware configuration including manipulators, end effectors, and other auxiliary welding equipments must be carefully calibrated, and the error rendered by thermal distortions is also difficult to be considered. In summary, any deviation in robotic accuracy, geometrical shapes of the welding seam, dimensions of workpiece, and thermal distortions would result in the computed welding path useless. Therefore, the adaptation or intelligence of the welding robot for various deviations in welding environment is still a key. This is exactly the motivation of this study. In this work, we develop an efficient and intelligent industrial double head welding robot with vision sensors for narrow seam tracking control. The welding robotic system is capable of sensing the instant status of seam during the welding process and controlling the torch to align the narrow seam immediately.

Currently, there are several existing methods, such as position-based visual servoing (PBVS) [14], image-based visual servoing (IBVS) [15], and hybrid visual servoing (HVS) [16], which can realize the seam tracking control of welding robots under the guidance of a vision system. For the PBVS and HVS systems, the complex vision sensor calibration is completed by designing a suitable calibration algorithm. As a result, the visual control precision is quite sensitive to the calibration errors in the PBVS and HVS systems. Moreover, the control method is generally used to deal with the bigger bias. For the control task of the little bias between narrow butt seam and torch, the IBVS is considered to be a more robust and effective strategy in dealing with camera and robot calibration errors [17–19]. Thus, the IBVS system has been employed in the field of narrow seam tracking via welding robots, such as container and laser welding [18, 19]. In particular, it was shown in [18] that the proposed real-time seam tracking algorithm can meet the accuracy demands of robotic laser welding. The Cartesian locations (position and orientation) measured by using vision sensors were added to the robotic trajectory during the robot motion. The simulation results demonstrated that the real-time seam tracking procedure is well suited for welding of moderately curved seam trajectories, and the tracking accuracy (0.1–0.5 mm) can be reached. In [20], the authors designed a welding manipulator to perform the butt-welding operation automatically for cylindrical sheet metals that are widely used in natural gas and heating systems. However, during the welding process, various disturbances and weak seam feature captured by the vision sensor would lead to instability of the seam feature extraction and tracking control. In order to reduce the effect of disturbances, the paper [13] presented a real-time planar butt seam tracking system with visual sensors for robotic manipulators. A kind of auto-regressive with exogenous input model was employed to describe the relationship between the rectifying voltage and offset. Then, a fuzzy proportional integral derivative (PID) seam tracking controller was designed by taking into account various offsets based on the ARX model. The experiment in [13] showed that most of the offsets can be controlled in the range of ±0.3 mm. In [21], the authors presented a method for the robust identification and location of three-dimensional (3D) narrow welding seams, achieving a robotic welding via an active laser vision. The results of [21] illustrated that the method can provide a 3D Cartesian accuracy within 1 mm—the range that is acceptable in most of the robotic arc welding applications. Notably, the laser visual sensor may not be suitable in tracking the narrow seam because the deformed laser light stripe for narrow seam is hard to be captured and recognized during the welding. To address this issue, the paper [22] presented a passive vision-based robotic welding system, which can effectively achieve the seam tracking function for pulse-MAG welding. The experimental results reported in [22] demonstrated that a satisfactory straight line and curved line seam can be achieved.

Although the vision-based seam tracking methods or systems reviewed so far have provided effective solutions to certain seam tracking problems, they certainly have limitations. Indeed, they can only be applied under some special conditions or environments. In this paper, we focus our attention on the situation where the narrow seam on the production line is presented. We develop an integrated vision control system that includes the initial point

positioning function, reasonable system design, and real-time seam tracking method to meet the demands of reliable, real-time, and fast-paced welding.

The rest of the paper is organized as follows. A double head welding robot configuration with the vision control system is presented in "The system configuration of welding robot with visual module" section. A fast and robust seam image processing algorithm is proposed in the "Seam image processing method" section. In the "Design of a visual servo control system" section, an image-based visual servo control system of industrial welding robot is designed for tracking butt narrow joint. Experimental results and implementations with the real industrial robots on container production line are given in the "Experimental results and analysis" section to verify the effectiveness of the proposed method. The "Conclusion" section contains conclusions of this study, summarizes the key point, and discusses future important applications.

2 The system configuration of welding robot with visual module

An industrial welding robotic system with visual measure and control function contains an industrial computer with touch screen, a digital camera, a lens, an electrical and control box, a three-axis robot, and other welding supporting facility, as shown in Fig. 1. The welding robot consists of three orthogonal sliders in the *x*-, *y*-, and *z*-axes. *Y*-axis is the welding direction.

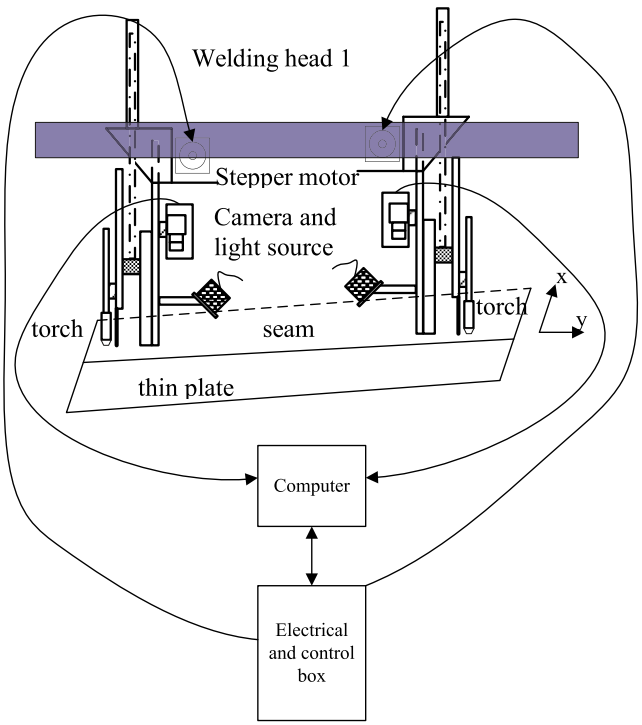

Fig. 1 A double head welding robotic system structure with visual servo control unit

The deviation between torch and seam can be eliminated in the *x*-axis direction by using a stepper motor. The distance between welding torch and plate plane in the vertical direction can be adjusted manually. The slider of *z*-axis is fixed on the slider of *x*-axis. The vision sensor is mounted on the slider of *z*-axis through a bracket, which can rise or fall in the two position of vertical direction under the control of pneumatic cylinder. There is a stepper motor at each end of the two axes, which can eliminate the deviation between seam and torch. The vision sensor consists of a CCD camera and a white light-emitting diode (LED) light source. The camera is installed ahead of the welding torch by a fixed distance, and its viewing direction is kept the same as the torch. The white LED light forms bright zone in the view field of the camera, which is convenient to generate a stable seam feature.

Remark: The laser sensor to tracking the seam is not considered because the seam is so narrow, and the deformed laser light stripe is hard to be captured and recognized reliably during the welding.

In Fig. 1, the welding head represents the moving part of the industrial robot during the welding process, which consists of the slider of *x*- and *z*-axes, vision sensor, light source, welding torch, and wire feed mechanism. It is noticed that the advantage of the double welding head is reflected in two aspects. Firstly, it can meet welding speed requirements in the rapid pace production line. Secondly, the good double side welding seam shape quality can be reached rapidly and reliably by implementing only one welding in one side.

During the running period of the welding robot system, the double welding head moves from both sides toward the center. When two heads meet, one stops and quickly moves back to its initial position; the other one continues to move forward to the stop position of the first one so as to complete the welding task. After the welding process is finished, the other welding head quickly moves back to its initial position to wait another welding process.

When two welding heads work during the welding process, the seam image is captured by the digital camera and then transferred to the industrial computer with touch screen through the USB interface. The image processing algorithm is implemented in the high performance computer. The extracted seam features including lines and points can be also displayed in the touch screen so as to monitor the process status. A seam image processing software with a friendly man–machine interface developed by our team is installed and run in the computer. The computer communicates with the programmable logic controller (PLC) through a RS232 port. When the PLC requests the seam feature data, the computer would immediately send the data to the PLC to realize online vision control. In order to ensure data reliability under the welding strong interference environment, the fieldbus protocol (Modbus) with data validation is used.

The electrical and control box includes a power supply system, motor driver, stepper motor, and main PLC. The PLC's outstanding merits are very reliable and safe. Thus, it is selected as the main controller of the visual servo control system. When the vision system works, the PLC requests and receives the image errors from the computer, computes the needed control input by using the proposed vision control algorithm and outputs them to the stepper motor driver. Then, the stepper motor is driven by the calculated control input so as to adjust the bias between measured seam and torch in the *x*-axis.

3 Seam image processing method

The seam image is captured by using the digital camera under white LED light irradiation during the welding. One typical weld seam image during the welding process is shown in Fig. 2, the other one before the welding process is shown in Fig. 3. Through the comparison of the two images, it can be seen clearly that many disturbances exist such as fume, arc light, and splash in Fig. 2. Thus, the weak narrow weld seam features are submerged into these disturbances. Moreover, the left and right presser feet lines also bring some difficulties for robustly and reliably extracting the feature of narrow weld seam.

In addition, image processing of the narrow seam need be completed in a short time in order to provide a real-time control function. Since the welding production of thin plate adopts CO_2 gas shielded arc welding mode, various disturbances exist and deteriorate the image quality, and hence making a real-time extraction of the seam feature rather difficult. Therefore, how to extract, in a robust and precise manner, the image features in the harsh environment is crucial in implementing the visual servo control method below for narrow seam tracking.

The seam image processing method including the following four steps will be designed to extract the image features reliably and quickly: (1) image pre-processing, (2) obtaining region of interest (ROI), (3) seam feature extraction, and (4) feature verification.

Fig. 2 Image during the welding

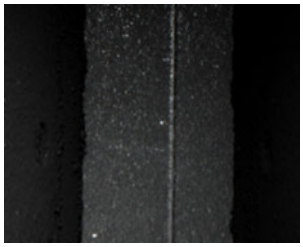

Fig. 3 Image before the welding

3.1 Image preprocessing

3.1.1 Linear transformation of seam image

Due to the influence of the ambient lighting during the robotic welding, the gray value of the seam image is uneven. Thus, the following linear transformation is used and operated on the whole image to improve the distribution of the gray value.

$$I(i,j)=\begin{cases}0, & I(i,j)<\alpha\\ \dfrac{(I(i,j)-\alpha)*255}{\beta-\alpha}, & \alpha\le I(i,j)\le\beta\\ 255, & I(i,j)>\beta\end{cases} \quad (1)$$

where $I(i,j)$ is the gray value of the pixel (i,j), α and β are two threshold values of the linear transformation which is used for adjusting the distribution of the grey value. In general, the two threshold values can be selected based on experts' experience.

3.1.2 Noise suppression of the seam image

During the welding with CO_2 gas shielded, strong arc welding, splashes, and smog have influences on the images. The strong noises can be found in the images of welding seam during the welding process. However, the arc light and splashes have the characteristic of instantaneity. Thus, most of the splashes generated in a sampling period will be disappeared in the next period. Based on this physical phenomenon, the disturbances can be removed by the following "min" operation on the last and current images.

$$I(i,j,t)=\min[I(i,j,t),I(i,j,t-1)] \quad (2)$$

where $I(i,j)$ is the gray values of pixel point (i,j) at the current time t, i and j are integers with $0<i\le W$, $0<j\le H$, H and W are the height and width of the images in the pixel.

For the other noises in the image, a median filter is employed to partly eliminate them. The median filter is a nonlinear spatial filter whose basic principle is based on an ordering of the pixels. In median filtering, the pixel values in the neighborhood window are ranked according to intensity, and the middle value becomes the output value for the pixel under evaluation. The median filter is very effective in reducing impulse noise during the welding. After completing the image preprocessing operation, most of the noises can be

removed, as illustrated in Fig. 4. This step is a key for the next step of the image processing.

3.2 Selection of the region of interest

During the image processing and feature extraction, the acquired digital seam image can be considered as a pixel array with the size of $H \times W$. By doing so, it brings not only a bigger computational burden to the seam image processing but also sacrifices the real-time performance of the vision system. To reduce the computational cost and shorten the image processing time, an ROI with H rows and F columns of pixels should be selected prior to the next step.

To obtain an effective ROI, the binary image processing operation for the weld seam is first implemented. After obtaining the binary seam image, all the pixel values are only two statuses, "0" and "1". Consequently, the ROI area can be accurately ensured by computing the sum of pixel values along with the vertical direction in the whole image. A detailed procedure is given below:

Step 1. Computing the sum of pixel value of each row by using the formula

$$L_r(j) = \sum_{i=1}^{H} I(i,j)/255, 1 \le j \le W \tag{3}$$

where $L_r(j)$ represents the sum of pixel value of each column in the binary seam image with H rows and W columns, whose distribution is shown by the blue curve in Fig. 5. In addition, h_1 and h_2 in Fig. 5 represent the left and right coordinates of intersection line between thin plate and presser feet.

Step 2. Search a local minimum value of $L_r(j)$ when the j is set in the range $[h_1, h_2]$ and the subscript corresponding to the local minimum is named by h_0;

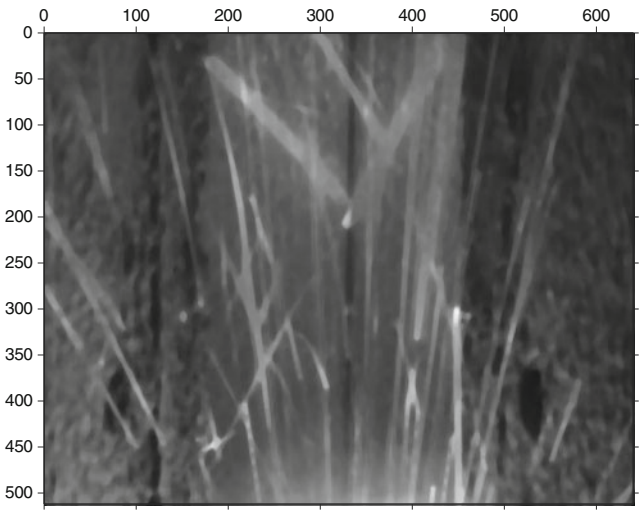

Fig. 4 The seam image after preprocessing

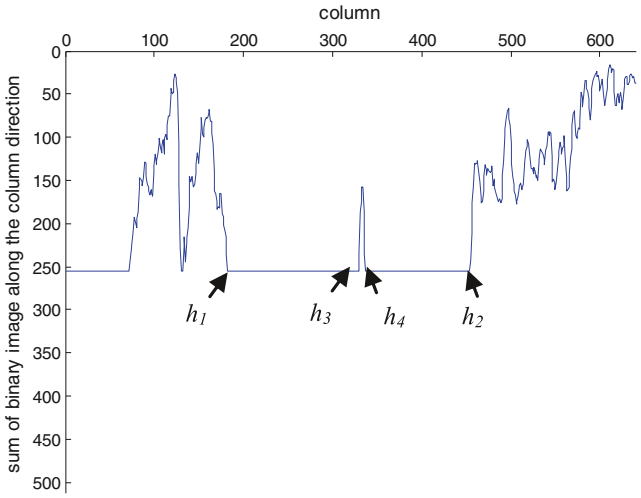

Fig. 5 The seam image distribution after preprocessing

Step 3. Set $i=h_0$. If $L_r(i)-L_r(i+1)>0$, then $i=i-1$. When $L_r(i)-L_r(i+1)=0$, define $h_3=i$;

Step 4. Set $i=h_0$. If $L_r(i)-L_r(i+1)>0$, then $i=i+1$. When $L_r(i)-L_r(i+1)=0$, define $h_4=i$;

Step 5. The ROI area is given by

$$\text{ROI} = I(i,j), h_3 \le j \le h_4 \tag{4}$$

where h_3 and h_4 represent the edge position of the ROI, and $F=h_4-h_3$.

After the ROI has been obtained, the width of processing image is F. Hence, the burden of calculation is reduced to F/W of the original one, which can remarkably enhance the computation efficiency and reduce the disturbance effects.

3.3 Seam line extraction

In order to realize the extraction of the narrow welding seam, the following actions, namely, profile extraction, Hough transform, and least-square fitting will be taken.

3.3.1 Profile extraction

After the vision system configuration is designed, the seam image would present the characteristics that the pixels in the welding seam are darker than the others along the row direction of the images after preprocessing. The gray distribution of seam binary image after preprocessing is given by Fig. 5. Its horizontal axis indicates the u-coordinates of the pixel points, and its vertical axis denotes their sum values along v-axes. The gray value of seam area is smaller than the others in the middle zone along the horizontal direction in the seam ROI image. To gain the seam profile along the

horizontal direction, we calculate the operator in the horizon direction as follows:

$$S_i = \frac{1}{2m+1}\sum_{i=-m}^{m} I(r+i, c+j) \tag{6}$$

where the variables r and c are selected to $r+i$ and $c+j$, respectively, so that they are greater than zero. The variable "m" is selected based on the width of the ROI seam, and the variable S_i represents the detection operator of seam pixel coordinates. It is worth noticing that Eq. (6) acts like a mean filter in one direction. Hence, the noise variance in the seam image is reduced by a factor of 2 m+1. In contrast to the Gaussian filter, the mean filter is preferable here because the Gaussian filter requires a larger filter mask for the same noise reduction and hence, leads to a longer execution time.

All the points that belong to the welding seam can be acquired by searching the image row by row with Eq. (6), as shown by the red points in Fig. 6. Clearly, there are some false points that do not belong to the welding seam. To obtain an accurate seam line and reduce the disturbance of feature points on the seam profile, the Hough transform and least-square fitting method will be employed.

3.3.2 Obtaining accurate line parameters

In the obtained seam profiles, the Hough transform is applied to extract the seam line from the profile points of narrow welding seam, as shown in Fig. 6. The angle from the v-axis to a line is represented by θ. The distance from the origin of image coordinates to a point in the profile is defined as ρ. Thus, the line parameters can be expressed as (ρ, θ) in the polar coordinates. The resolution of the parameter θ in the polar coordinates is set to 1° to accelerate the algorithm, and the range of θ is limited between 0–5 and 175–180° by considering the fact that the seam is placed in the rectangular copper tank of welding robot whose size is about 10 × 2,500 mm.

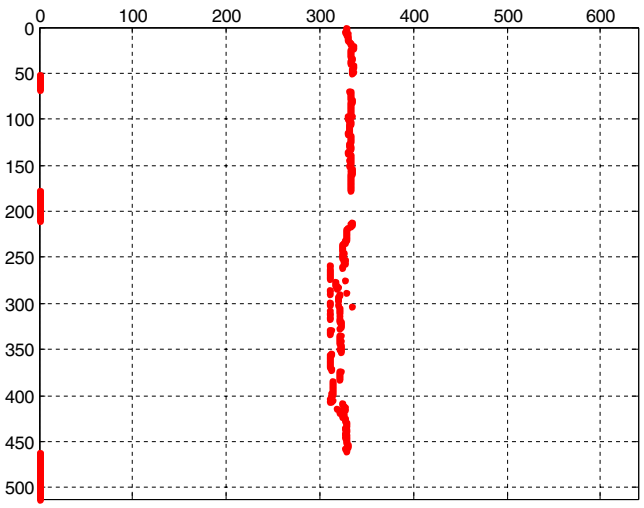

Fig. 6 The pixel coordinates of seam profiles

However, it should be noted that the parameters of the seam line obtained by the Hough transform are not very accurate. Since it is important to correctly and precisely determine the feature lines for the vision control system, a statistical method is also employed to determine the candidates of the feature line from many frames of seam image. After the welding starts, a group of frames of valid seam images is chosen to get the candidates of feature line. The feature line in i-th valid image is extracted by the Hough transform as described in the "Profile extraction" section, and is denoted as (ρ_i, θ_i), i=1, 2, …, K.

It is assumed that two sets of parameters are subject to a normal distribution. Then, a three-sigma rule may be used to verify the effectiveness of the seam feature. If the rule is satisfied, nearly all of the parameters values (99.73 %) lie within three standard deviations of the parameters.

ρ is accepted, only if

$$P_\rho\left(\mu_\rho - 3\sigma_\rho \le \rho \le \mu_\rho + 3\sigma_\rho\right) \ge 0.9973 \tag{7}$$

θ is accepted, only if

$$P_\theta\left(\mu_\theta - 3\sigma_\theta \le \theta \le \mu_\theta + 3\sigma_\theta\right) \ge 0.9973 \tag{8}$$

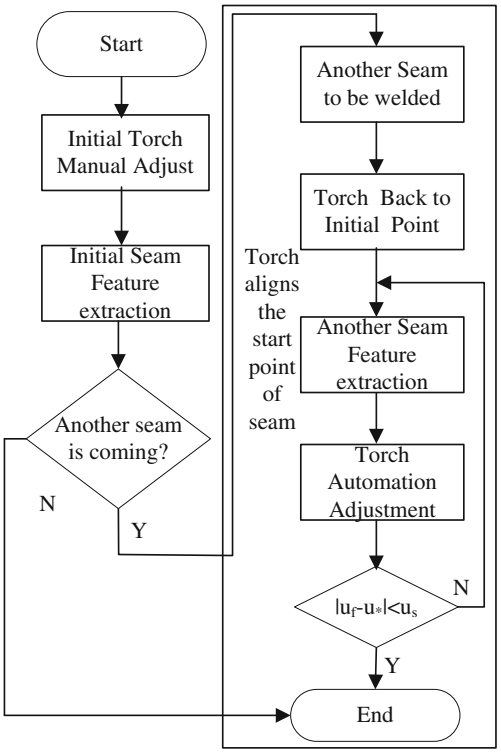

Fig. 7 A procedure of torch automation position at the start point

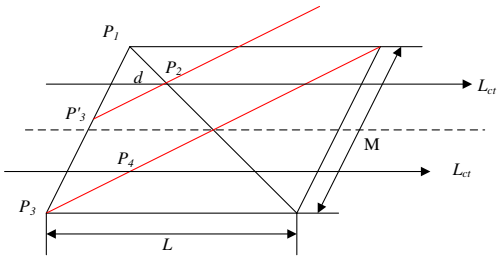

Fig. 8 A spatial geometric relationship with the maximum error

where μ_ρ, μ_θ is the mean of the parameter ρ_i, θ_i, respectively, $\sigma_\rho, \sigma_\theta$ is the standard deviation of the parameter ρ_i, θ_i. ρ and θ denote the new measured line parameters, P_ρ, and P_θ denote the probability of the new measured line parameters, respectively. Hence, ρ and θ are effective and accepted when Eqs. (7) and (8) hold simultaneously. The line parameters ρ and θ, can then be used as a standard line that are helpful in determining the candidate points as well as in computing the accurate center line.

3.3.3 Accurate seam line extraction

In order to reduce the measurement error of feature points of the seam line and enhance the reliability of seam line recognition, the least-square technique and Hough transform are used to get the accurate center line of the seam. If the distance from a point on the centering line obtained by the Hough transform is less than a preset threshold, it is accepted as a

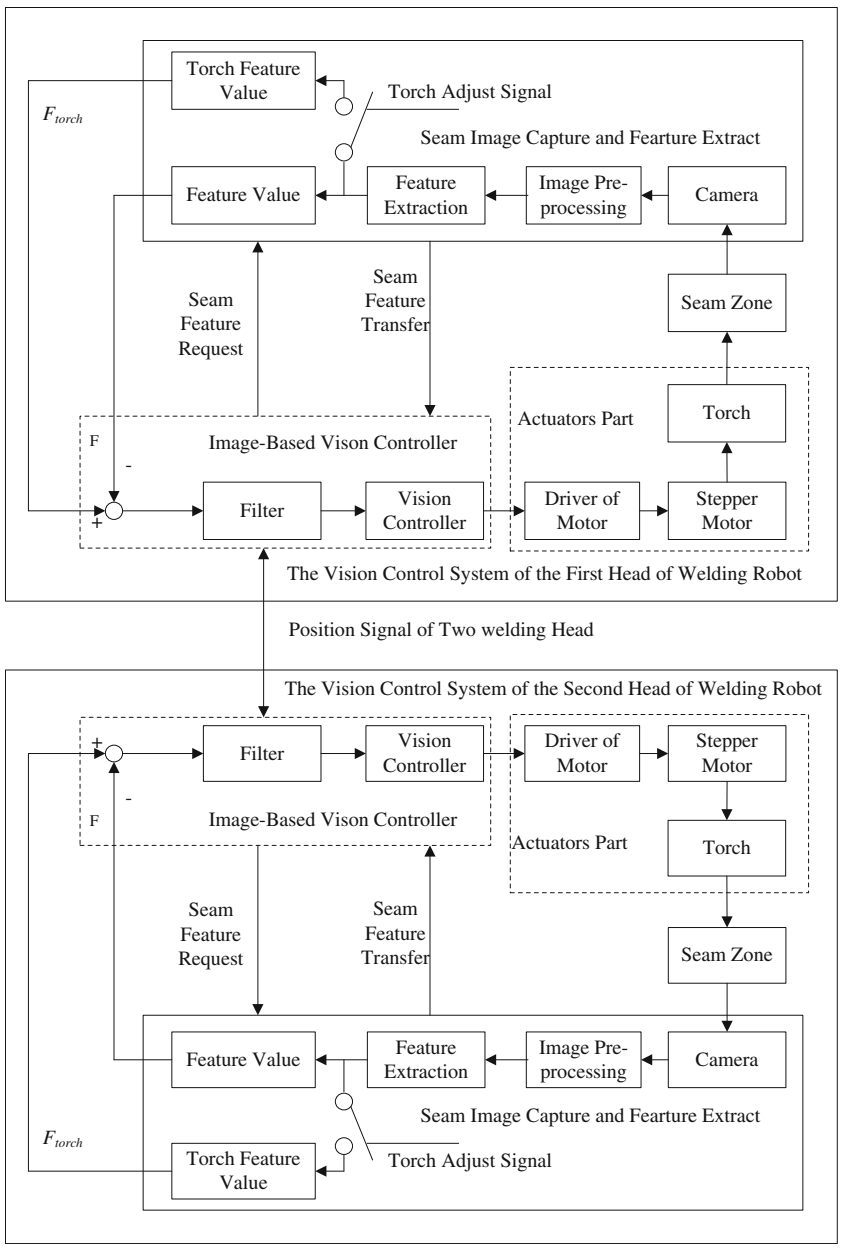

Fig. 9 The image-based vision controller in the double head welding robot

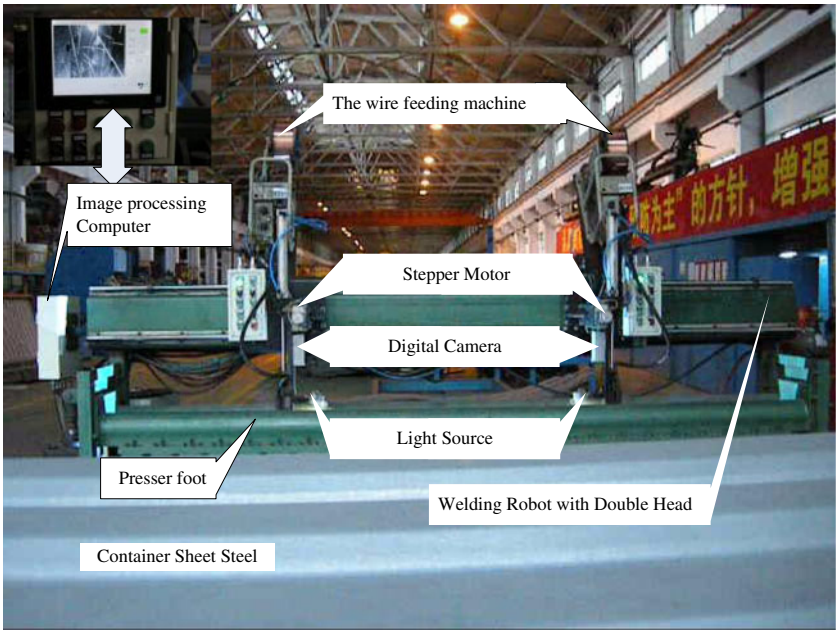

Fig. 10 An industrial double head welding robot with vision system

candidate point. Then, a least-square fitting is applied to the candidate points to compute the accurate centering line, as shown in Eqs. (9)–(11).

$$u = a_0 + a_1 v \tag{9}$$

where a_1 is the slope of the extracted seam line in image plane, a_0 is intercept of the line in image plane.

$$\begin{aligned} a_0 &= \overline{u} - a_1 \overline{v} \\ a_1 &= \frac{\sum_{i=1}^{N} u_i v_i - N\overline{u}\,\overline{v}}{\sum_{i=1}^{N} v_i^2 - N\overline{v}} \end{aligned} \tag{10}$$

$$\left(\overline{u}, \overline{v}\right) = \left(\frac{1}{N}\sum_{i=1}^{N} (u_i), \frac{1}{N}\sum_{i=1}^{N} (v_i)\right) \tag{11}$$

where (u_i, v_i) are the image coordinates of the i-th candidate point, N is the number of the candidate points, and ($\overline{u}$, $\overline{v}$) are the average image coordinates of the candidate points, and (u, v) are the image coordinates of the point on the seam line.

Fig. 11 The vision control system

Since the v-coordinate of the intersection point of the horizontal midline and the seam line is selected as the image feature, we substitute v in Eq. (9) with $0.5H$ and get the image feature by

$$u_f = a_0 + a_1 H/2 \tag{12}$$

where u_f is the u-coordinate of the feature point, H is the height of the seam image. Since the v-coordinate of the feature point lies in the optical center of the camera, it ensures the smallest distortion about the u-coordinate of the feature.

3.4 Feature verification

Although the feature points can be obtained by using the aforementioned method, it is inevitable that there are errors in the image features. In fact, it is hard to ensure that the extracted image features are correct because of the influences of the strong noises in the real-time welding process. If they are directly utilized as feedback signals in the visual servo

Table 1 Performance parameters of the welding robot

Parameters	Description
Measure scale	0.06 mm/pixel
Control scale	25 pulses/pixel
Control period	0.1 s
Controller	K_p=0.4, K_i=0.08, K_d=0.005
Welding type	CO_2 gas-shielded arc welding
Welding width	0.1 mm
Seam length	1,980 mm
Welding speed	1,000 mm/s

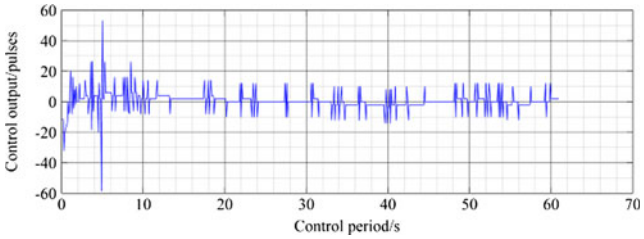

Fig. 12 The control pulse curve of the first welding head

control system, the torch would depart from the welding seam quickly. As a result, the aim of narrow seam tracking may not be reached. Thus, the feature verification is necessary.

In our application, the seam line lies in the range of a rectangular copper tank, and can be guaranteed by workers or a mechanical positioning system. Thus, the physical constraint condition can be used to verify the effectiveness of the extracted feature.

4 Design of a visual servo control system

For the implementation of the image-based visual servo control scheme, three conditions must be satisfied: (1) a desired torch feature in the image plane can be obtained; (2) the current seam feature in the image plane is made available; and (3) a fast, reliable, and robust visual control method can be developed. The automatic positioning procedure of torch at the start point and real-time seam tracking during the welding can be accomplished by using the described three-step procedure.

4.1 Torch automation position at the start point

The relationship between the position of the torch and the corresponding image feature is shown in Fig. 1. The selection procedure of the torch feature point and the adjustment of a starting position are given by the following diagram.

When the torch is replaced or cleaned up due to a damage or blockage, the start position of torch must be recalibrated. A robotic system can ensure that the torch is back to the start position in the next welding cycle. At this position, the weld feature in each welding cycle is selected as the torch feature point. Then, the torch automation adjustment can be finished by using the torch feature points, the seam feature in each welding cycle, and control method. In order to evaluate the effectiveness of such a method, the start point positioning error will also be analyzed.

In Fig. 7, u^* is a desired torch feature point, u_f is the weld seam feature, and u_s is a predefined constant. According to the practical robotic system configuration and the welding operation technique of narrow seam, the following spatial geometric relationship between a camera and torch with the maximum error is considered, as shown in Fig. 8.

In order to understand the spatial geometric relationship, the following assumptions are made through this paper.

1. The width of a rectangular copper groove is M, and the length of the thin sheet steel to be welded is L;
2. The straight line L_{ct} is parallel to the u-axis in the image plane;
3. The distance between the torch and optical axis of camera is represented by d; and
4. The straight lines P_1P_2 and P_3P_4 are both located in the allowable position range.

When the maximum error of the start point of seam exists, the different seam should lie in the two diagonal line positions according to the geometry position relation between a torch, camera, and copper groove. Thus, after the start position of torch is calibrated, the torch aligns the point P_3, and the computed seam feature is the point P_4. When another seam to be welded is well placed under the welding torch and the camera, the torch will be back to the initial torch position and the corresponding seam feature is the point P_2. According to the initial position adjustment step, the torch position will be adjusted to P'_3 from P_3 by using the vision control method and the two seam features, e.g., P_2 and P_4. Hence, the distance error $P_1P'_3$ always exists. According to the principle of the similar triangles, the adjust error can be represented as

$$\frac{P_e/2}{M/2} = \frac{d}{L/2} \tag{13}$$

where P_e is the distance between point P_1 and point P'_3. The Eq. (13) can be rewritten as

$$P_e = 2 * d * M/L \tag{14}$$

where M is a constant in the practical application, L is related to the size of thin sheet steel and is known. Thus, the parameter d decides the localization accuracy of torch at the start position. In conclusion, through a suitable selection of the parameters d and M, a desired maximum localization error can be controlled by using the torch automation procedure at the start point.

4.2 Visual controller

Due to a large number of arc interference, splash, camera calibration errors, robot modeling errors, and vibration errors

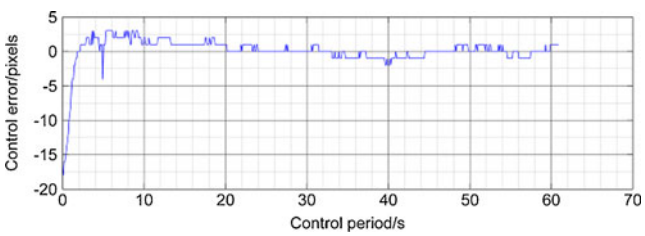

Fig. 13 The seam tracking error of the first welding head

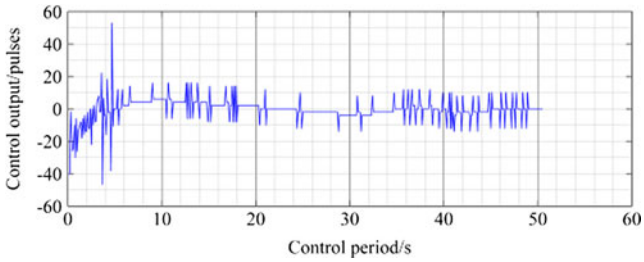

Fig. 14 The control pulse curve of the second welding head

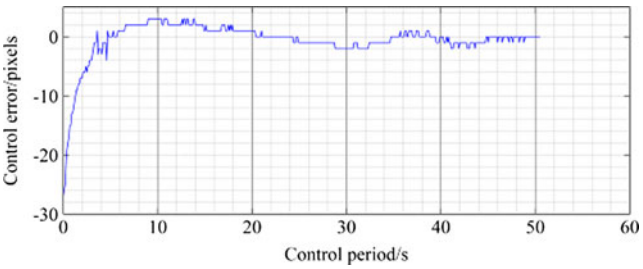

Fig. 15 The seam tracking error of the second welding head

always exist during the welding. A controller will be designed by using the image-based visual control method that is robust and capable of attenuate the disturbances. Moreover, the PLC is used as the main controller and a digital camera as the vision sensor. The PLC is widely used in industries, whose reliability is well acknowledged. Compared with conventional analog cameras, a digital camera has a more reliable embedded digital signal processor.

The structure of the proposed controller is shown in Fig. 9. It primarily consists of three parts: seam image capture and feature extraction, actuators module, and image-based vision control. The seam image capture and feature extraction are used to sense the seam bias and provide feedback signals of the closed-loop vision controller. Moreover, it also provides the desired image feature, e.g., torch feature value, after the initial torch adjustment is completed. Its operation is controlled by the PLC and sends a request to the camera, while the vision sensor system sends the extracted image feature to the PLC. The PLC can accomplish three important functions, i.e., image error filtering, PID controller realization, and output pulse control for the motor driver. In particular, it sends requests to the vision sensor system for image features, and then computes the needed pulses based on the feedback image features and controller algorithm, and outputs pulses to the driver of stepper motor. In addition, the PLC also receives operational signals from panel and another welding head.

The image error between the reference and current features is proportional to the distance that the welding torch differs from the welding seam. On the other hand, the adjusted distance of the welding torch is proportional to the driven pulses sent to the stepper motor. Thus, the scale from the driven pulses to the moved distance in the pixel of image can be estimated before welding. It can be merged into the parameters of an incremental PID controller of the form

$$\Delta p(k) = S\left\{\begin{array}{l} K_p[e(k)-e(k-1)] + K_i e(k) + \\ K_d[e(k)-2e(k-1)+e(k-2)] \end{array}\right\} \quad (15)$$

where $\Delta p\ (k)$ is the output of the PID controller in the k-th control period; $e\ (k)$ is the filtered image error of the period; and K_p, K_i, and K_d are the proportional, integral, and differential gains, respectively. S is the pulse equivalent, i.e.,

$$S = \Delta p / \Delta d \quad (16)$$

where Δd is the distance between the reference and current points in the image plane, and Δp is the pulse numbers in the Cartesian frame that can drive the current image feature to the reference image feature.

5 Experimental results and analysis

To achieve the fast welding pace required by the container production line, an industrial welding robot with double heads is developed, which can shorten the welding time and enhance efficiency of the production line. To test the performance of the proposed visual servo control method for narrow butt joint, experiments have been conducted in the industrial robot, as shown in Fig. 10. The welding robot system with double heads is composed of two electric welding machines, two wire feed mechanisms, two vision control systems, two torches, two cameras, two stepper motors, two presser foot mechanical systems, and two correction error mechanical systems.

The presser foot pressed the workpiece on the two sides of the welding seam to avoid heat deformation and vibration disturbances. The torch can be automatically aligned to the initial welding seam position before welding by using the proposed torch automation position algorithm.

To facilitate the operation of the visual servo control system, a vision control system shown in Fig. 11 is designed. It is

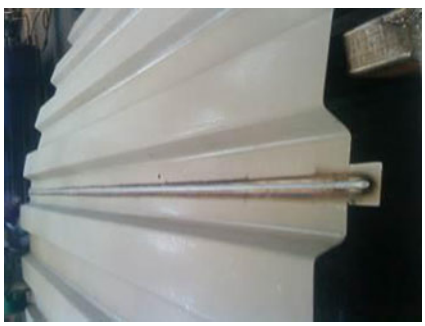

Fig. 16 The good formed seam

composed of a computer with a touch screen, a PLC controller, a stepper motor driver, auxiliary electric units, and various control buttons. The vision control system can realize many important functions, such as seam video image capture, image processing and feature extraction, communication, localization control of the torch at starting point, and real-time seam tracking control.

A set of parameters of the vision control system are listed in the following Table 1, under which a desirable control performance is achieved.

After the welding starts, the two welding heads move from both sides toward the center. In Figs. 12 and 13, the welding time is 61 s, while the welding time in Figs. 14 and 15 is 51 s. When the two welding heads meet at 51 s, one stops welding and quickly moves back to its initial position, the other one still moves forward to the stop position of the first welding head after 10 s to complete the weld task of the whole seam.

During the welding, the two torches in the welding heads are firstly adjusted to the start position of seam, as shown in Figs. 13 and 15 In Fig. 13, the welding torch position deviating from the weld is about 18 pixels. The large bias can be quickly adjusted to about 1 pixel in 3 s. By comparison, the welding torch position deviating from the weld is about 24 pixels in Fig. 15, and the larger bias can be adjusted to about 1 pixel in 3.6 s. In fact, the vision control process during the initial 3 s is the seam start point adjustment process.

After the torch is aligned to the seam initial position, the welding process and real-time seam tracking start immediately. In Figs. 12 and 14, it can be seen that the maximum tracking error is 3 and 4 pixels, respectively. According to the calibration of camera system, the error range is about 0.3 and 0.4 mm, respectively. The corresponding control curves are shown in Figs. 12 and 14, respectively. Clearly, the range of the control lies in small intervals. It can be rapidly transferred to the driver of the motor and executed by stepper motor. As a result, a real-time seam tracking is realized, as illustrated in Figs. 13 and 15. Figure 16 demonstrates that the desired welding quality is obtained.

6 Conclusion

A short welding time is one of the key performances for welding robots in production line. In this paper, a welding robot with double heads has been employed to improve the welding efficiency and quality of narrow seam on the rapid container welding production line. The double head welding robot can better meet the welding requirement, namely, a good double side welding seam shape is desired by implementing only one welding. Moreover, the image-based vision servo control method is used to achieve the starting position control and real-time seam tracking for the welding robot in the rapid container welding production line. The welding robot with a visual servo control system can meet the challenges caused by the seam change and high welding speed, and significantly improve welding quality and production efficiency.

There are two reasons for not using a filter in the proposed vision sensor system. The first one is that the arc light and white LED light source are utilized to identify seam feature, which create a good image contrast during the welding process. The second reason is that a narrow seam feature cannot be reliably recognized by the camera if a filter is employed. Nevertheless, using the method proposed in this work, desirable results have been obtained as confirmed by the experiment.

In the near future, the need of the narrow seam welding will be increasing significantly, due to the wide applications of the high-strength sheet steel and the laser weld technology. The vision image processing and control method proposed in this paper can play an active role in meeting such demands and achieving the recognition and tracking of the narrow seam for various welding robots.

Acknowledgments This work was supported by the National Nature Science Foundation of China under Grant 61203275, Science and Technology Research Project of University in Hebei Province (YQ2013036) and the Natural Science Foundation of Hebei Province, China (F2014202071)

This work was also supported in part by 973 Program (2012CB215202), 111 Project (B08015), Key Lab on Wind Energy and Smart Grids (CXB201005250025A), and Research Projects (JC201105160551A), (KQC201105300002A) and (JCYJ20130329152125).

References

1. Heber M, Lenz M, Rüther M, Bischof H, Fronthaler H, Croonen G (2013) Weld seam tracking and panorama image generation for on-line quality assurance. Int J Adv Manuf Technol 65(9–12):1371–1382
2. Pan ZX, Polden J, Larkin N, Duin SV, Norrish J (2012) Recent progress on programming methods for industrial robots. Robot Comput Integr Manuf 28(2):87–92
3. Bi ZM, Lang SY (2007) A framework for CAD- and sensor-based robotic coating automation. IEEE Trans Ind Inform 3(1):84–91
4. Chen SB, Qiu T (2004) Intelligentlized technologies for robotic welding. Ser Lect Notes Control Inf Sci 299:123–143
5. Xu D, Fang ZJ, Chen HY, Yan ZG, Tan M (2012) Compact visual control system for aligning and tracking narrow butt seams with CO_2 gas-shielded arc welding. Int J Adv Manuf Technol 62(9–12):1157–1167
6. Kim JY (2007) CAD-based automated robot programming in adhesive spray systems for shoe out soles and uppers. J Robot Syst 21: 625–634
7. Bae KY, Park JH (2006) A study on development of inductive sensor for automatic weld seam tracking. Mater Process Technol 76(1–3): 111–116
8. Eskandari S, Arezoo B, Abdullah A (2013) Positional, geometrical, and thermal errors compensation by tool path modification using three methods of regression, neural networks, and fuzzy logic. Int J Adv Manuf Technol 65(9–12):1635–1649
9. Gao XD, Na SJ (2005) Detection of weld position and seam tracking based on Kalman filtering of weld pool images. J Manuf Syst 24(10):1–12
10. Ge JG, Zhu ZQ, He DF, Chen LQ (2005) A vision-based algorithm for seam detection in a PAW process for large-diameter stainless steel pipes. Int J Adv Manuf Technol 26(9–10):1006–1011

11. Kuo HC, Wu LJ (2002) An image tracking system for welded seams using fuzzy logic. Mater Process Technol 120(1–3): 169–185
12. Tsai MJ, Lee HW, Ann NJ (2011) Machine vision based path planning for a robotic golf club head welding system. Robot Comput Integr Manuf 27(4):843–849
13. Ma H, Wei S, Sheng Z, Lin T, Chen SB (2009) Robot welding seam tracking method based on passive vision for thin plate closed-gap butt welding. Int J Adv Manuf Technol 48(9–12):945–953
14. Mahajan A, Figueroa F (2007) Intelligent seam tracking using ultrasonic sensors for robotic welding. Robotica 15(3):275–281
15. Wilson WJ, Hulls CC, Bell GS (1996) Relative end-effector control using Cartesian position-based visual servoing. IEEE Trans Robot Autom 12(5):684–696
16. Mariottini GJ, Oriolo G, Prattichizzo D (2007) Image-based visual servoing for nonholonomic mobile robots using epipolar geometry. IEEE Trans Robot 23(1):87–100
17. Allibert G, Courtial E, Chaumette F (2010) Predictive control for constrained image-based visual servoing. Robot IEEE Trans 26(5): 933–939
18. Graaf M, Aartsa A, Jonkera B, Meijera J (2010) Real-time seam tracking for robotic laser welding using trajectory-based control. Control Eng Pract 18(8):1–10
19. Zhang WZ, Chen Q, Zhang GX, Sun ZG, Du D (2007) Seam tracking of articulated robot for laser welding based on visual feedback control. Rob Weld Intell Autom Lect Notes Control Inf Sci 362:281–287
20. Özcan M (2011) Determining seam profile tracking of very narrow butt welding on sheet metal. Sci Res Essays 6(23):5040–5048
21. Dinham M, Fang G (2013) Autonomous weld seam identification and localisation using eye-in-hand stereo vision for robotic arc welding. Robot Comput Integr Manuf 29(5):288–301
22. Ye Z, Fang G, Chen SB, Zou JJ (2013) Passive vision based seam tracking system for pulse-MAG welding. Int J Adv Manuf Technol 67(9–12):1987–1996